



# Nitrogen-doped graphene quantum dots doped silica nanoparticles as enhancers for electrochemiluminescence thrombin aptasensors based on 3D graphene

Fangkai Du<sup>1</sup> · Hui Zhang<sup>1</sup> · Xuecai Tan<sup>1</sup> · Chenhao Ai<sup>1</sup> · Mengru Li<sup>1</sup> · Jun Yan<sup>1</sup> · Min Liu<sup>1</sup> · Yeyu Wu<sup>1</sup> · Defen Feng<sup>1</sup> · Shaogang Liu<sup>1</sup> · Heyou Han<sup>1,2</sup>

Received: 31 March 2019 / Revised: 19 July 2019 / Accepted: 20 July 2019 / Published online: 30 July 2019  
© Springer-Verlag GmbH Germany, part of Springer Nature 2019

## Abstract

A sensitive electrochemiluminescence (ECL) aptasensor based on 3D graphene is described for thrombin detection utilizing nitrogen-doped graphene quantum dots doped silica (NGQDs@SiO<sub>2</sub>) nanocomposite labeling as an enhancer. Ru(bpy)<sub>3</sub><sup>2+</sup>-Pt nanoparticles (Ru-PtNPs) with an ECL signal were dropped onto a 3D graphene-modified electrode, and then, a complementary thrombin aptamer (cDNA) was conjugated to the Ru-PtNPs. Finally, NGQDs@SiO<sub>2</sub>, coupled with the thrombin aptamer as the booster, was attached to the electrode surface by using hybridization with the cDNA, and the ECL intensity was efficiently enhanced. The target thrombin induced the NGQDs@SiO<sub>2</sub> nanocomposites labeled with the thrombin (TB) aptamer to be extracted because of their strong binding with thrombin. The immobilization amount of NGQDs@SiO<sub>2</sub> on the modified electrode decreased. Thus, the presence of thrombin could result in a decrease in the ECL signal. On the basis of the signal amplification factors, the fabricated ECL aptasensor demonstrated excellent properties with concentrations varying from 2.0 pM to 50 nM and a detection limit of 23.1 fM.

**Keywords** Graphene quantum dots · Electrochemiluminescence · 3D graphene · Aptasensor · Thrombin

## Introduction

Graphene quantum dots (GQDs), as an emerging star in the carbon nanomaterial family [1], have drawn enormous attention due to their robust chemical inertness and alluring properties, such as good biocompatibility, functional flexibility,

excellent cell membrane permeability, and ideal optical properties [2–6]. To increase certain properties of GQDs, research has focused on heteroatom doping modifications of GQDs [7, 8]. Therefore, the fabrication, performance, and application of nitrogen-doped GQDs (NGQDs) have become a popular research focus [9]. In recent years, NGQDs with excellent fluorescent properties have been developed for bioimaging [10], sensors [11], and electrocatalytic activity [12]. Furthermore, luminescent methods have been combined with electrochemical techniques to expand NGQD-based sensing applications. Up to now, several electrochemiluminescence (ECL) sensors based on NGQDs have been reported [13–18]. Despite the significant aforementioned progress in ECL sensing, there is still room for improvement in the available sensors for application such as improving their water solubility, simplifying the modification processes, and generating a high or stable ECL signal for NGQDs.

Thrombin, as a specific serine protease, plays a vital role in blood agglomeration. It can promote soluble fibrinogen to convert to insoluble fibrin and subsequently form the fibrin gel for clots [19, 20]. The thrombin concentration level in the blood is closely related to several coagulation

Fangkai Du and Hui Zhang contributed equally to this work.

**Electronic supplementary material** The online version of this article (<https://doi.org/10.1007/s10008-019-04352-z>) contains supplementary material, which is available to authorized users.

✉ Xuecai Tan  
gxunxctan@126.com

<sup>1</sup> Guangxi Key Laboratory of Chemistry and Engineering of Forest Products, Key Laboratory of Guangxi Colleges and Universities for Food Safety and Pharmaceutical Analytical Chemistry, School of Chemistry and Chemical Engineering, Guangxi University for Nationalities, Nanning 530008, People's Republic of China

<sup>2</sup> State Key Laboratory of Agricultural Microbiology, College of Science, College of Food Science and Technology, Huazhong Agricultural University, Wuhan 430070, People's Republic of China

abnormalities, and it can serve as a biomarker for tumor diagnosis [21, 22]. Accordingly, the highly sensitive detection of thrombin is critical and useful in disease prevention [23, 24]. Electrochemiluminescence (ECL), a kind of electrochemical analytical technique, has attracted significant interest owing to its advantages such as a low background signal, low detection limit, the use of a cheap and simple optical setup, and high sensitivity [25, 26]. Recently, some solid-state ECL sensors have been designed for chemical and biological species detection because the solid-state ECL analysis is superior to solution-phase analysis with respect to the reduction in expensive reagent consumption, enhancement of the ECL signal, and simplified experimental design [27, 28]. However, the immobilization method of the solid-state electrode might decrease the conductivity, which would limit its application. To improve the ECL intensity and electroconductibility, nanoparticles have been widely adopted as carriers in ECL sensors. Three-dimensional (3D) graphene has been used as an ideal carrier because of its excellent conductivity, high specific surface area, and porous structure to facilitate the access of analyte and electrolyte [29, 30]. Moreover, Pt nanoparticles are an excellent labeling material in ECL sensors because of their safety, sensitivity, and stability [31].

On the other hand, aptamers are single-strand DNA or RNA oligonucleotides that have the specific ability of binding to targets, such as some small organic molecules and RNA enzymes [32]. The excellent properties of aptamers promote exploration into their application in the wide range of electrochemiluminescence biosensing, since they are superior to those of traditional antibodies because of aptamers' smaller size, better thermal and chemical stability, increased stability, and easier synthesis [33, 34]. The ECL aptasensors show high sensitivity and selectivity, readily available instrumentation, and favorable application in biosensing [35–38]. For example, Sun's group has fabricated a sandwiched ECL aptasensor for the detection of TB based on a sensitive and 3D nitrogen-doped graphene oxide with a detection limit of 0.25 fM, which provides a promising potential for the study of bimolecular and early diagnosis of diseases [38].

Herein, an ECL aptasensor for the determination of thrombin was fabricated with a newly designed model platform constructed by the self-assembly of DNA-functionalized NGQDs and 3D graphene. For this sensor, Pt nanoparticles (PtNPs), which increased the ECL signal of  $\text{Ru}(\text{bpy})_3^{2+}$ , were used to provide a high surface area for the hybridization of NGQDs. On the basis of the synergism of NGQDs and 3D graphene, an intense ECL signal was observed. In the presence of thrombin, NGQDs@ $\text{SiO}_2$ -labeled TB aptamers were extracted due to their strong binding with thrombin, thus resulting in a decrease in the ECL signal. This strategy provides a new insight into expanding the ECL application of NGQDs.

## Experimental

### Materials and reagents

Chloroplatinic acid ( $\text{H}_2\text{PtCl}_6$ ) was provided by Sinopharm Chemical Reagent (Shanghai, China). Graphite powder was purchased by Beilian Chemical Company (Tianjin, China). L-cysteine concentrated sulfuric acid, phosphoric acid,  $\text{KMnO}_4$ , 3-thiophene malonic acid, N-(3-dimethylaminopropyl)-N-ethylcarbodiimide hydrochloride (EDC), and N-hydroxysuccinimide (NHS) were ordered from Aladdin Biological Technology (Shanghai, China). Tris(2,2'-bipyridyl)dichlororuthenium(II) hexahydrate ( $\text{Ru}(\text{bpy})_3\text{Cl}_2 \cdot 6\text{H}_2\text{O}$ ), Nafion (5 wt%), tetraethyl orthosilicate (TEOS), and 3-thiophenemalonic acid were purchased from Adamas-Beta (Shanghai, China). Triton X-100 (TX-100) was purchased from Biosharp (Hefei, China). Bovine serum albumin (BSA) and thrombin (TB) were supplied by Sigma-Aldrich (Madrid, Spain). Immunoglobulin G (IgG) and hemoglobin (Hb) were ordered from Solarbio Science and Technology (Beijing, China). Lysozyme was acquired from Kang Biological Technology (Jiangsu, China). The thrombin aptamers (TBA) and complementary DNA (cDNA) were freshly prepared from Cowin Biotech (Beijing, China), and the corresponding sequences are described as follows:

TBA: 5'- $\text{NH}_2$ -( $\text{CH}_2$ )<sub>6</sub>-TTTTTTGGTTGGTGTGGTTGG-3'  
cDNA: 5'-SH-( $\text{CH}_2$ )<sub>6</sub>-CCAACCACACCAACC-3'

The water used all throughout the experiments was purified by a Millipore platform.

### Apparatus

The fluorescence and UV-Vis absorption spectra were obtained through a Hitachi F-4600 spectrophotometer and Agilent Cary60 UV-Vis spectrophotometer, respectively. An MPI-EII model electrochemiluminescence analyzer was employed to record the ECL signals with a PMT voltage of 600 V. The electrochemical experiments were carried out on a CHI 660E electrochemical workstation (Chenhua Apparatus Co., Ltd., China). All the electrochemical experiments were performed with a three-electrode system containing a glassy carbon electrode (GCE, 3-mm diameter) as the working electrode, a platinum pole electrode as the auxiliary, and an Ag/AgCl electrode as the reference electrode. Scanning electron microscopy (Carl Zeiss SUPRA 55 Sapphire, Germany) and transmission electronic microscopy (TEM) (JEM-2010HR, Japan) were used to characterize morphology and size of the synthetic materials.

### Synthesis of 3D graphene

Based on the study by Marcano [39], graphene oxide (GO) was prepared by using Hummers' method. In brief, 1.0 g of

graphite powder and 13.3 mL of phosphoric acid were added to 70 mL of concentrated sulfuric acid with stirring at 0 °C. Then, 6.0 g of potassium permanganate was added to the mixture. The obtained mixture solution was heated at 50 °C for another 12 h, giving a dark-brown solution. The reaction mixture was poured into ice water containing 30% H<sub>2</sub>O<sub>2</sub>. The resultant yellow GO suspension was filtered, and the residue was washed successively with water, 30% HCl, and ethanol. The 3D graphene was synthesized by heating 10 mL of an aqueous dispersion containing GO (1.8 mg mL<sup>-1</sup>) and L-cysteine (5 mg mL<sup>-1</sup>) in a Teflon-lined autoclave at 200 °C for 12 h [40]. After cooling to room temperature, the mixture was washed by deionized water three times and freeze-dried to acquire the 3D graphene. Then, the solid was redispersed in an ethanol solution containing 5% Nafion with a final concentration of 1.0 mg mL<sup>-1</sup>.

### Preparation of Ru(bpy)<sub>3</sub><sup>2+</sup>-Pt nanoparticles (Ru-PtNPs)

Ru-PtNPs were prepared according to previous literature [41]. First, 1 mL of 0.3 M 3-thiophene malonic acid was added to 100 mL of an H<sub>2</sub>PtCl<sub>6</sub> (0.76 mmol L<sup>-1</sup>) aqueous solution and then heated at 100 °C for 20 min to give Pt nanoparticles (PtNPs). Subsequently, 0.038 mmol Ru(bpy)<sub>3</sub>Cl<sub>2</sub> was dissolved in 1 mL of water and dropped into 50 mL of the as-formed PtNP solution under vigorous stirring. The reaction suspension was then centrifuged at 8000 rpm for 20 min, and the residue of the resultant Ru-PtNPs was redispersed in different concentrations in an ethanol:water = 1:1 (v:v) solution and stored at 4 °C for further use.

### Preparation of the NGQDs

NGQDs were synthesized according to the previous literature with appropriate modifications [42]. Citric acid (25 mg) was dissolved in 12.5 mL of water, 500 µL ammonia was quickly added, and the solution was stirred well. Then, the solution was sealed in a Teflon-lined autoclave (20 mL) and treated at 200 °C for 3 h. When cooling down to 25 °C, the dark-brown solution was collected using a 0.22-µm polyethersulfone membrane and dialyzed (molecular weight cutoff of 3500 Da) with a dialysis bag against purified water for 24 h. The NGQs were stored for further use.

### Preparation of the NGQDs@SiO<sub>2</sub>

The preparation of NGQDs@SiO<sub>2</sub> was based on a previous study [43]. Briefly, 4.0 mL of H<sub>2</sub>O, 10.0 mL of ethanol, and 2.0 mL of ammonia were first put into a beaker. Subsequently, ethoxy silane (100 µL) was rapidly added to the solution. The mixture was vigorously stirred until equilibrium was reached at room temperature to give a good distribution. Afterwards,

the silica particle dispersion was centrifuged, washed several times with ethanol, and dried under vacuum.

To prepare NGQDs@SiO<sub>2</sub> composites, 8.0 mL of a SiO<sub>2</sub> nanoparticle (12.5 mg mL<sup>-1</sup>) ethanol suspension was mixed with APTES (1.0 mL) with continued stirring for 6 h. Then, the dispersion was centrifuged and washed with ethanol five times to give amino-functionalized SiO<sub>2</sub> nanoparticles. Afterwards, the resultant SiO<sub>2</sub> nanoparticles were introduced into the mixture solution of 1.0 mL of the as-formed NGQDs and 1.0 mL of EDC (10 mg mL<sup>-1</sup>), which was stirred for 12 h at 4 °C. The NGQDs@SiO<sub>2</sub> composites were generated after centrifugation and washing several times with water and then dispersed in 1.0 mL total volume of water for subsequent experiments.

### Preparation of the NGQDs@SiO<sub>2</sub>/TBA

The obtained SiO<sub>2</sub>@NGQDs dispersion (0.5 mL) described above was treated with TBA (0.5 mL, 500 µmol L<sup>-1</sup>) solution. Then, 200 µL of newly obtained EDC (20 mg mL<sup>-1</sup>) and 200 µL NHS (10 mg mL<sup>-1</sup>) were added to the suspension, which was stirred for another 2 h to obtain the NGQDs@SiO<sub>2</sub>/TBA complexes. The products were washed with PBS solution (pH of 7.4) and then dispersed in 1.0 mL (pH of 7.4) PBS solution and stored at 4 °C for subsequent use.

### Preparation of TB aptasensor

The fabrication procedure of the aptasensor for detecting TB is demonstrated in Scheme 1. The procedure is described as follows. Initially, the Nafion 3D graphene was dropped onto precleaned electrodes. Subsequently, the as-prepared Ru-PtNPs (5.0 µL) was coated on the modified electrode and incubated for 25 min. Then, 20 µL of cDNA (1.5–2.2 µM) was linked to the modified electrode, and incubation continued for 15 h at 4 °C. The electrode was then soaked in 0.1% BSA solution for 30 min to block unbound active sites. Finally, 20 µL of the prepared NGQDs@SiO<sub>2</sub>/TBA composites was dropped onto the electrode surface, and incubation continued for 2 h. After washing with PBS buffer (pH of 7.4), the resultant ECL aptasensor was stored at 4 °C for subsequent use.

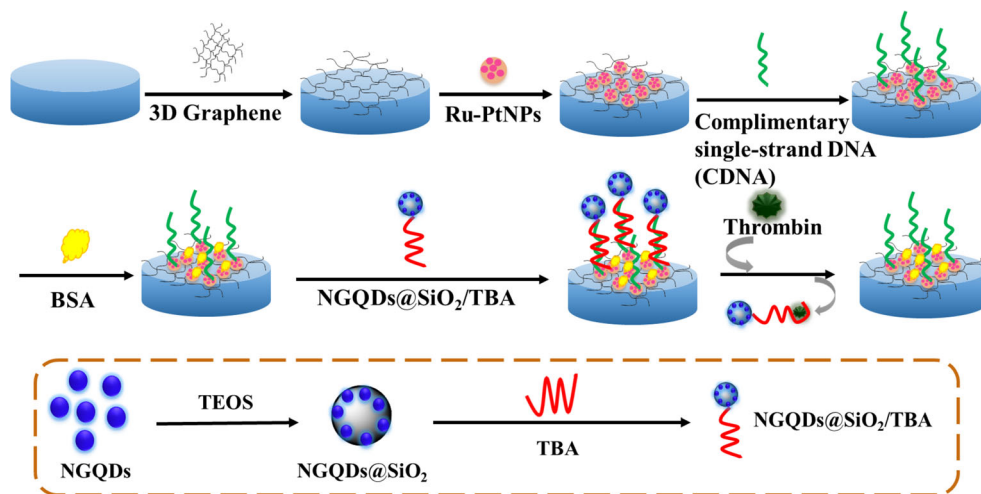
## Results and discussion

### Characterization of the prepared nanocomposites

The morphology of the synthesized 3D graphene was characterized by SEM and TEM. The SEM image (Fig. 1a) shows a view of 3D graphene oxide nanosheets with typical wrinkles and ripples as well as the partial overlapping and stacking. The corresponding TEM image (Fig. 1b) further confirms this result. The as-prepared



**Scheme 1** Illustration of the preparation of the aptasensor for the detection of thrombin



PtNPs and Ru-PtNPs were investigated using TEM. As illustrated in Fig. 1c, PtNPs with a diameter of approximately 2 nm exhibited a spherical morphology, suggesting that the PtNPs were successfully prepared. After hybridization with Ru(bpy)<sub>3</sub><sup>2+</sup>, a number of dots appeared on the amorphous surface (Fig. 1d), indicating the successful preparation of Ru-PtNPs. To further confirm the gradual synthesis of Ru-PtNPs, the UV-Vis spectra of PtNPs,

Ru(bpy)<sub>3</sub><sup>2+</sup>, and Ru-PtNPs are included in Electronic Supplementary Material (ESM) Fig. S1 for comparison. It was found that the UV-Vis spectrum of Ru-PtNPs exhibited characteristic absorption peaks at 241 nm, 287 nm, and 455 nm, which is ascribed to the Ru(bpy)<sub>3</sub><sup>2+</sup>. Additionally, a typical broad absorption almost crossing the entire UV-visible light region for the PtNPs can also be seen in the UV-Vis spectrum of Ru-PtNPs.

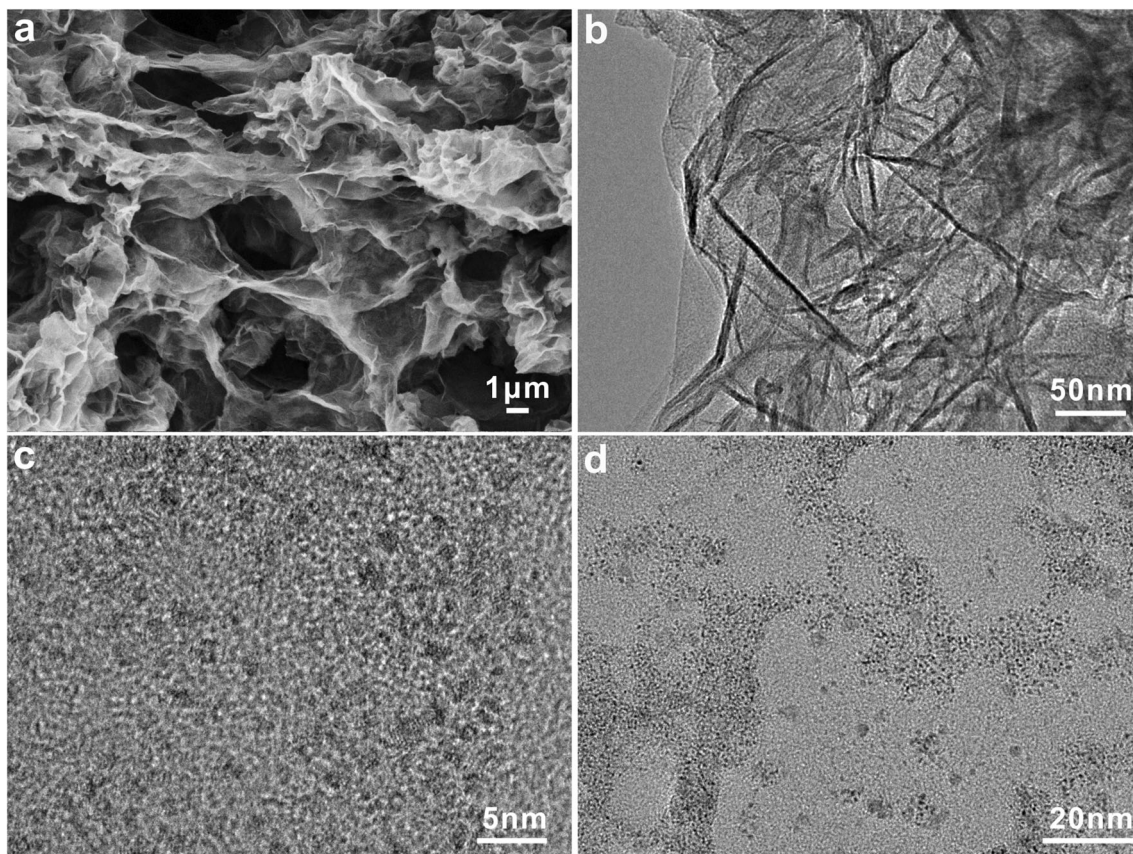


**Fig. 1** SEM image of 3D graphene (a). TEM images of 3D graphene (b), PtNPs (c), and Ru-PtNPs (d)

Additionally, the FL spectrum of the Ru-PtNPs exhibited an optimal maximum emission wavelength at 610 nm, which was assigned to the characteristic emission peak of Ru(bpy)<sub>3</sub><sup>2+</sup> (Fig. S1B). The results prove the successful fabrication of Ru-PtNPs.

The prepared NGQs were characterized with different techniques, as shown in Fig. 2. The TEM observation reveals that the NGQs are well dispersed with a size of approximately 6 nm, as shown in Fig. 2a. In addition, the spectroscopic and optical characteristics of the NGQDs were evaluated. The absorption spectrum of the NGQDs shows an absorption band located at approximately 230 nm and a peak at approximately 345 nm (Fig. 2b). The absorption band at approximately 230 nm was attributed to the aromatic  $\pi$ - $\pi^*$  transition [44]. The strong peak located at 345 nm demonstrates a typical absorption band of C-N and is attributed to the  $n$ - $\pi^*$  transition of C-N, further suggesting the doping with N elements [45]. The fluorescence spectrum in Fig. 2b illustrates that NGQs exhibit a maximum emission at 440 nm with an excitation wavelength of 345 nm. Meanwhile, the aqueous NGQDs display a strong blue photoluminescence under a 365-nm UV lamp (inset of Fig. 2b).

In addition, the morphologies of NGQDs@SiO<sub>2</sub> and NGQDs@SiO<sub>2</sub>/TBA nanocomposites were investigated by SEM. Figure 2c displays that the as-produced NGQDs@SiO<sub>2</sub> exhibited a spherical morphology with an average size of ca. 130 nm. After coating with the TBA, the surface of the NGQDs@SiO<sub>2</sub> nanocomposite was filled with flocc (Fig. 2d). Furthermore, the UV-Vis absorption spectrum of NGQDs@SiO<sub>2</sub>/TBA nanocomposites was measured (Fig. S2), which showed two characteristic absorption peaks; one peak located at 262 nm was the characteristic absorption of TBA and another centered at 336 nm was the characteristic absorption of NGQDs. Accordingly, the FT-IR spectrum of NGQDs@SiO<sub>2</sub>/TBA nanocomposites also contained both the characteristic absorption peaks of NGQDs@SiO<sub>2</sub> and TBA (Fig. S3). These results indicated NGQDs@SiO<sub>2</sub>/TBA nanocomposites were successfully prepared.

The proposed sensor was characterized by UV-Vis and FT-IR. As depicted in Fig. S4, the sensor (3D graphene/Ru-PtNPs/cDNA/BSA/ NGQDs@SiO<sub>2</sub>/TBA) revealed absorption peaks at 463 nm and 261 nm, which contributed to Ru-PtNPs and cDNA, respectively. Accordingly, the FT-IR spectrum of the sensor also contained both the characteristic absorption peaks of NGQDs@SiO<sub>2</sub>/TBA and 3D graphene/Ru-

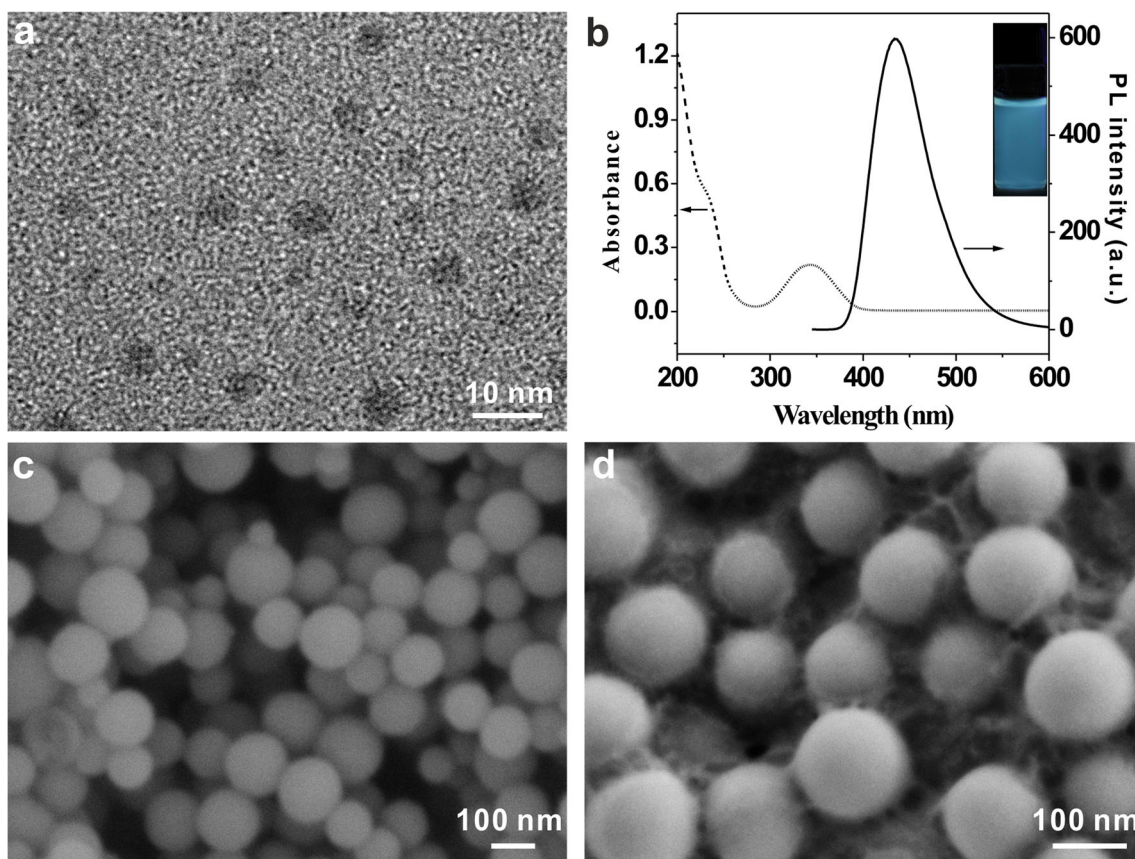


**Fig. 2** **a** TEM image of NGQDs. **b** UV-Vis absorption spectrum and fluorescence spectrum of NGQDs (the inset shows the photograph of the NGQDs under excitation at 365 nm). SEM images of **c** NGQDs@SiO<sub>2</sub> and **d** NGQDs@SiO<sub>2</sub>/TBA



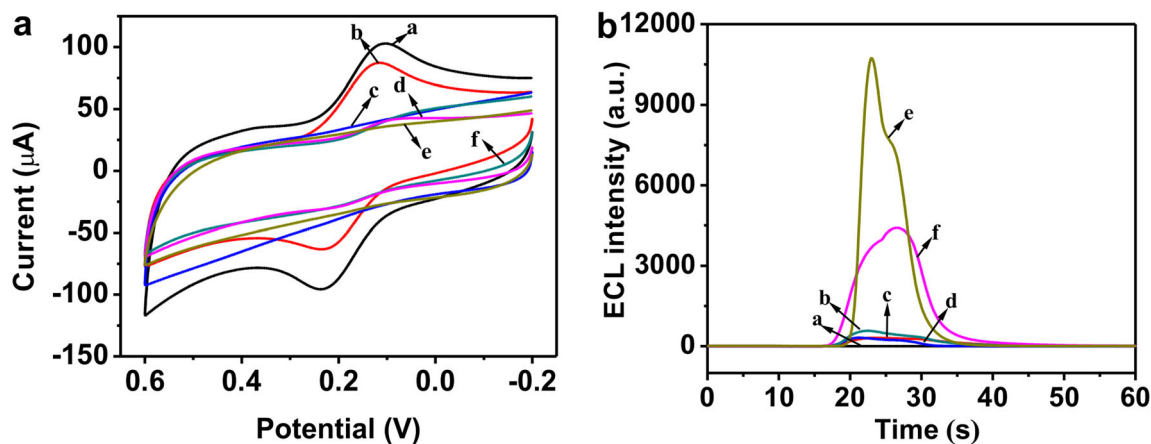


**Fig. 3** **a** CVs of 3D graphene (a), 3D graphene/Ru-PtNPs (b), 3D graphene/Ru-PtNPs/cDNA (c), 3D graphene/Ru-PtNPs/cDNA/BSA (d), 3D graphene/Ru-PtNPs/cDNA/BSA/NGQDs@SiO<sub>2</sub>/TBA (e) modified GCEs and the proposed aptasensor incubated with  $1 \times 10^{-8}$  mol L<sup>-1</sup> thrombin (f) in 0.1 mol L<sup>-1</sup> PBS (pH of 7.4) containing 0.1 mol L<sup>-1</sup> KCl and 5 mol L<sup>-1</sup> K<sub>4</sub>Fe(CN)<sub>6</sub>/K<sub>3</sub>Fe(CN)<sub>6</sub>. **b** The ECL of 3D graphene

(a), 3D graphene/Ru-PtNPs (b), 3D graphene/Ru-PtNPs/cDNA (c), 3D graphene/Ru-PtNPs/cDNA/BSA (d), 3D graphene/Ru-PtNPs/cDNA/BSA/NGQDs@SiO<sub>2</sub>/TBA (e) modified GCEs and the proposed aptasensor incubated with  $1 \times 10^{-8}$  mol L<sup>-1</sup> thrombin (f) in 0.1 mol L<sup>-1</sup> PBS (pH of 7.4)

PtNPs/cDNA/BSA, such as peaks located at 3400, 1642, and 1388 cm<sup>-1</sup> of NGQDs, and located at 1626, 798 cm<sup>-1</sup> of Ru-PtNPs (Fig. S5). Evidently, these results confirm the successful fabrication of the sensor.

### CV and ECL of the ECL aptasensor

Cyclic voltammetry (CV) was used to further evaluate the construction of the sensing platform, as shown in Fig. 3a.

The 3D graphene-modified GCE displayed an apparent redox current (curve a). When the Ru-PtNPs were coated onto the surface of the 3D graphene-modified electrode, the reduction peak current decreased (curve b). This result was ascribed to the thickness of the electrode surface which hinders the electron transfer. With the interaction between amino groups and PtNPs, the incorporation of the amino group determined cDNA onto the modified electrode greatly reduces the redox current (curve c). Afterwards, BSA was adopted to block

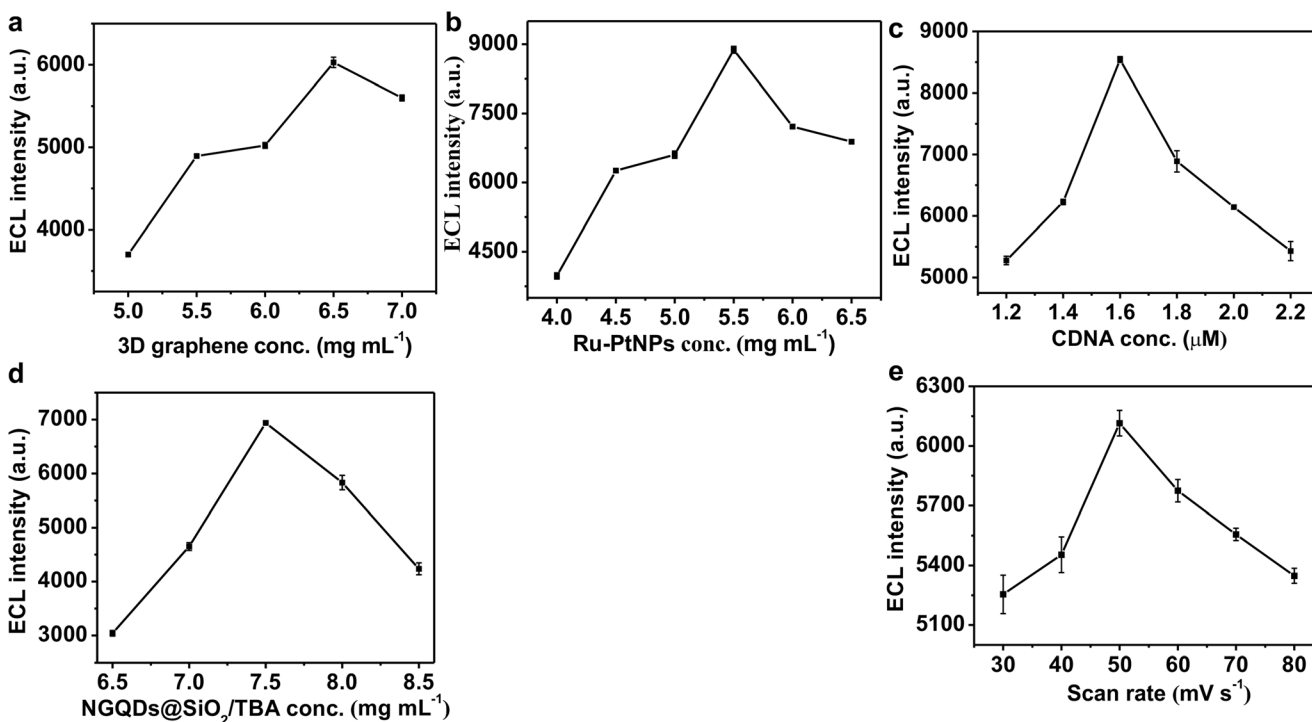


**Fig. 4** Effect of **a** the amount of 3D graphene, **b** the amount of Ru-PtNPs, **c** the amount of cDNA, **d** the amount of NGQDs@SiO<sub>2</sub>/TBA, and **e** the scan rate on the ECL intensity

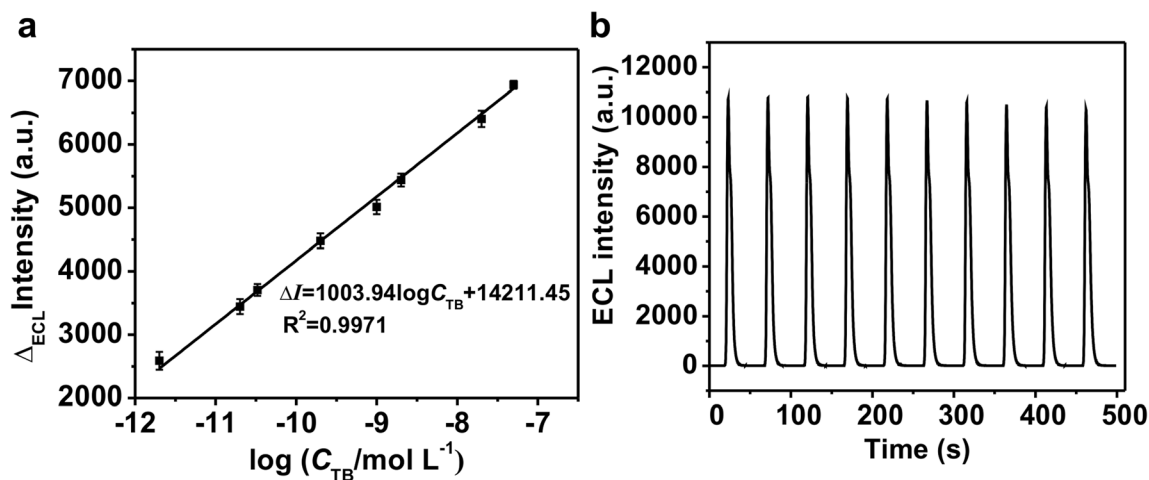
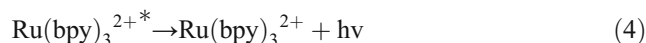
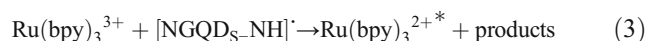
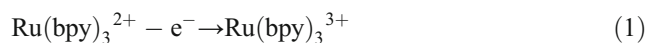


**Fig. 5** **a** The calibration plot against the corresponding  $\log C_{TB}$ . **b** Stability of ECL signal from aptasensor in phosphate buffer 0.1 M (pH 7.4) under a continuous cyclic potential scan for 10 cycles

possible nonspecific active sites, further inducing a decrease in the redox current (curve d). After the immobilization of the TBA-labeled NGQDs@SiO<sub>2</sub> through base-pairing interactions, the redox current was further decreased (curve e). The ECL aptasensor was then immersed in a 10-nM thrombin solution, and an enhancement in redox current was acquired (curve f). This could be attributed to the TBA-labeled NGQDs@SiO<sub>2</sub> that were extracted due to their stronger binding with thrombin, reducing the amount of NGQDs@SiO<sub>2</sub> and hindering the electron transfer of the aptasensor. All these phenomena demonstrated each layer of the film was successfully fabricated on the electrode.

To test the electrochemiluminescence properties of the developed sensor, ECL measurements were performed, as depicted in Fig. 3b. No signal in ECL intensity could be found for the 3D graphene-modified GCE electrode (curve a). After anchoring Ru-PtNPs on the surface of the electrode, the ECL signal increased gradually (curve b). It is rational to assume that cDNA and BSA anchored on the surface of electrode can reduce the intensity of the ECL signal (curves c and d) [46]. Then, the TBA was hybridized with the cDNA to introduce the NGQDs@SiO<sub>2</sub> onto the modified electrode, and a large increase in the ECL signal was achieved. This result occurs because the NGQDs@SiO<sub>2</sub> reveals a strong amplification of the

Ru(bpy)<sub>3</sub><sup>2+</sup> ECL. After the addition of TB, the TBA-labeled NGQDs@SiO<sub>2</sub> segment was binding with thrombin by the specific TB-TBA interaction. As a consequence, a decrease in the ECL signal was observed because of the partial departure of NGQDs@SiO<sub>2</sub>. According to the reported literature [47], the ECL mechanism may be demonstrated as follows:



### Optimization of experimental conditions

The following parameters influencing the ECL response of the modified electrode were optimized, including the concentrations of 3D graphene, Ru-PtNPs, TBA, NGQDs@SiO<sub>2</sub>/TBA, and the scan rate. The corresponding data and figures are described in Fig. 4. According to Fig. 4, the abovementioned experimental parameters were demonstrated to obtain optimal results as follows: (a) the concentration of 3D graphene was

**Table 1** Comparisons with other methods for the determination of thrombin

Methods	Detection system	Linear range	Detection limit	Time	References
Microscale thermophoresis	MB-TBA1/Bio-TBA2/SA-PE	18-554 nM	5.4 nM	30 min	[48]
Fluorescence spectroscopy	AuNP/Apt29-1/Apt29-2/Probe DNA	0.625-50 nM	0.16 nM	150 min	[49]
Differential pulse voltammetry	Fc-TBA/Au	5.0-35 nM	0.5 nM	-	[50]
Electrochemical luminescence	Tri(bpyRu)-β-CD/Aptamer	1.0 pM-10 nM	0.1 pM	-	[51]
Electrochemical luminescence	3D graphene/Ru-PtNPs/cDNA/BSA /NGQDs@SiO <sub>2</sub> /TBA	2.0 pM-50 nM	23.1 fM	-	This work

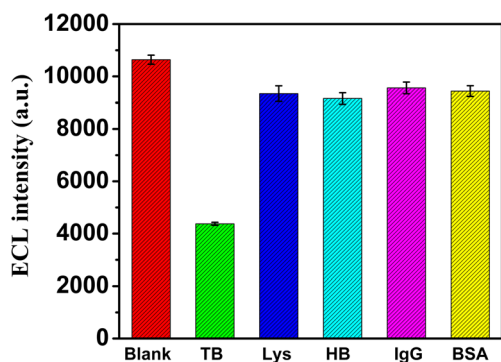


**Fig. 6** Selectivity tests for the ECL response of the aptasensor to thrombin, lysozyme, human hemoglobin, IgG, and BSA

6.5 mg mL<sup>-1</sup>, (b) the concentration of Ru-PtNPs was 5.5 mg mL<sup>-1</sup>, (c) the TBA concentration of the ECL aptasensor was 1.6 μM, (d) the NGQDs@SiO<sub>2</sub>/TBA concentration of the ECL aptasensor was 7.5 mg mL<sup>-1</sup>, and (e) the scan rate of the ECL aptasensor was 50 mV s<sup>-1</sup>.

### Determination of TB

Under the optimized conditions, the ECL aptasensor was constructed for detecting TB. As depicted in Fig. 5a, the integrated change of ECL intensity ( $\Delta_{\text{ECL}}$ ) exhibited a linear response to the logarithmic concentration of TB from  $2.00 \times 10^{-12}$  to  $5.0 \times 10^{-8}$  mol L<sup>-1</sup>, with a correlation coefficient of 0.9971. The linear regression equation was described as follows:  $\Delta_{\text{ECL}} = 1003.94 \times \log C_{\text{TB}} + 14211.45$  (mol L<sup>-1</sup>), and the lower detection limit was  $2.31 \times 10^{-14}$  mol L<sup>-1</sup> ( $S/N=3$ ). In addition, the analytical performance of the ECL aptasensor for the detection of TB is compared with that of other reported methods (Table 1). It is observed that the proposed aptasensor exhibited more excellent properties than did other methods.

### Repeatability, stability, and selectivity

To evaluate the repeatability of the developed ECL sensor, successive scanning measurements for ten cycles were

**Table 2** Determination of thrombin added in human serum with the proposed ECL aptasensor

Sample	Added (nM)	Found (nM) <sup>a</sup>	Recovery (%)	RSD (% , n = 3)
1	0.01	0.01026	102.6	2.56
2	0.5	0.488	97.6	3.27
3	2.5	2.44	97.5	2.33
4	20	20.2	101.0	4.56
5	40	42.6	106.5	3.61

<sup>a</sup> Each data was given as average value obtained from three successive determinations

performed, and the relative standard deviation (RSD) was 1.63% (Fig. 5b). In addition, the RSD for eight different electrodes constructed in the same way was 3.02%. Furthermore, the stability was also monitored at different time intervals. The results indicate that the ECL intensities maintained 93.61–94.6% of the original response after 15 days. Therefore, the sensor shows good repeatability and stability.

In addition to the aforementioned factors, the specificity is another vital criterion for the performance evaluation of the ECL sensor. It is evident that, as illustrated in Fig. 6, the ECL intensity of the aptasensor is significantly decreased upon the addition of TB, while the other interferents produce negligible decreases in the ECL intensity. The results indicated that the aptasensor has a high selectivity to TB.

### Thrombin detection in human clinical serum samples

To test the practicality and viability of the developed aptasensor, we evaluated the aptasensor's detection of TB in human serum. The serum samples were diluted 100 times prior to the measurements, and different amounts of thrombin were added. The results demonstrated acceptable quantitative recoveries between 97.5 and 106.5% (Table 2). The results make it feasible to utilize the developed aptasensor for the detection of TB in real samples.

### Conclusions

In summary, this work demonstrates an ECL aptasensor for sensing thrombin based on a 3D graphene/Ru-PtNPs/NGQDs@SiO<sub>2</sub>/TBA-modified electrode. The NGQDs were proven to enhance the ECL signal. Meanwhile, 3D graphene and PtNPs were used to accelerate the electron transfer, thus further improving the ECL signal. In addition, the ECL aptasensor exhibited satisfactory sensing properties, such as good selectivity, superior stability, good repeatability, and a low detection limit, thereby demonstrating its potential application for the detection of TB in biological systems.

**Funding information** This work was supported by the National Sciences Foundation of China (21365004), the Natural Science Foundation of Guangxi (2017GXNSFBA198026, 2018GXNSFAA294044, 2018GXNSFAA281136), the Key Research and Development Project of Guangxi (AB18126048), the Specific Research Project of Guangxi for Research Bases and Talents (AD18126005), the Basic Ability Enhancement Program for Young and Middle-aged Teachers of Guangxi (2018KY0168), the Scientific Research Foundation of Guangxi University for Nationalities (2016MDQD002), the High-Level-Innovation Team and Outstanding Scholar Project of Guangxi Higher Education Institutes, the Xiangsihu Young Scholars Innovative Research Team of Guangxi University for Nationalities, and the State Key Laboratory of Analytical Chemistry for Life Science, Nanjing University (SKLACL1810).



## References

- Tetsuka H, Asahi R, Nagoya A, Okamoto K, Tajima I, Ohta R, Okamoto A (2012) Optically tunable amino-functionalized graphene quantum dots. *Adv Mater* 24(39):5333–5338
- Baker SN, Baker GA (2010) Luminescent carbon nanodots: emergent nanolights. *Angew Chem Int Ed* 49(38):6726–6744
- Zhang Z, Zhang J, Chen N, Qu L (2012) Graphene quantum dots: an emerging material for energy-related applications and beyond. *Energy Environ Sci* 5(10):8869–8890
- Shen J, Zhu Y, Yang X, Li C (2012) Graphene quantum dots: emergent nanolights for bioimaging, sensors, catalysis and photovoltaic devices. *Chem Commun* 48(31):3686–3699
- Chowdhury AD, Ganganboina AB, Tsai YC, Chiu HC, Doong R.A (2017) Multifunctional GQDs-Concanavalin A@Fe<sub>3</sub>O<sub>4</sub> nanocomposites for cancer cells detection and targeted drug delivery. *Anal Chim Acta* 1027:109–120
- Zhou L, Lin Y, Huang Z, Ren J, Qu X (2012) Carbon nanodots as fluorescence probes for rapid, sensitive, and label-free detection of Hg<sup>2+</sup> and biothiols in complex matrices. *Chem Commun* 48(8):1147–1149
- Du Y, Guo S (2016) Chemically doped fluorescent carbon and graphene quantum dots for bioimaging, sensor, catalytic and photoelectronic applications. *Nanoscale* 8(5):2532–2543
- Li L, Wu G, Yang G, Peng J, Zhao J, Zhu JJ (2013) Focusing on luminescent graphene quantum dots: current status and future perspectives. *Nanoscale* 5(10):4015–4039
- Li Q, Zhang S, Dai L, Li L (2012) Nitrogen-doped colloidal graphene quantum dots and their size-dependent electrocatalytic activity for the oxygen reduction reaction. *J Am Chem Soc* 134(46):18932–18935
- Li W, Zhang Z, Kong B, Feng S, Wang J, Wang L, Yang J, Zhang F, Wu P, Zhao D (2013) Simple and green synthesis of nitrogen-doped photoluminescent carbonaceous nanospheres for bioimaging. *Angew Chem Int Ed* 52(31):8151–8155
- Liu XT, Na WD, Liu Q, Su XG (2018) A novel label-free fluorescent sensor for highly sensitive detection of bleomycin based on nitrogen-doped graphene quantum dots. *Anal Chim Acta* 1028:45–49
- Khonsari YN, Sun SG (2019) A novel label free electrochemiluminescent aptasensor for the detection of lysozyme. *Mater Sci Eng C* 96:146–152
- Chen HJ, Li W, Wang Q, Jin X, Nie Z, Yao SZ (2016) Nitrogen doped graphene quantum dots based single-luminophore generated dual-potential electrochemiluminescence system for ratiometric sensing of Co<sup>2+</sup> ion. *Electrochim Acta* 214:94–102
- Chen SF, Chen XQ, Xia TT, Ma Q (2016) A novel electrochemiluminescence sensor for the detection of nitroaniline based on the nitrogen-doped graphene quantum dots. *Biosens Bioelectron* 85:903–908
- Liu Q, Ma C, Liu XP, Wei YP, Mao CJ, Zhu JJ (2017) A novel electrochemiluminescence biosensor for the detection of microRNAs based on a DNA functionalized nitrogen doped carbon quantum dots as signal enhancers. *Biosens Bioelectron* 92:273–279
- Qi BP, Zhang XR, Shang BB, Xiang DS, Qu WY, Zhang SH (2017) A facile method to sensitively monitor chlorinated phenols based on Ru(bpy)<sub>3</sub><sup>2+</sup> electrochemiluminescent system using graphene quantum dots as coreactants. *Carbon* 121:72–78
- Tian KL, Li DJ, Tang TT, Nie F, Zhou Y, Du JX, Zheng JB (2018) A novel electrochemiluminescence resonance energy transfer system of luminol-graphene quantum dot composite and its application in H<sub>2</sub>O<sub>2</sub> detection. *Talanta* 185:446–452
- Nie GM, Wang Y, Tang Y, Zhao D, Guo QF (2018) A graphene quantum dots based electrochemiluminescence immunosensor for carcinoembryonic antigen detection using poly(5-formylindole)/reduced graphene oxide nanocomposite. *Biosens Bioelectron* 101:123–128
- Li Y, Liu L, Fang X, Bao J, Han M, Dai Z (2012) Electrochemiluminescence biosensor based on CdSe quantum dots for the detection of thrombin. *Electrochim Acta* 65:1–6
- Deng N, Liang Z, Liang Y, Sui Z, Zhang L, Wu Q, Yang K, Zhang L, Zhang Y (2012) Aptamer modified organic-inorganic hybrid silica monolithic capillary columns for highly selective recognition of thrombin. *Anal Chem* 84(23):10186–10190
- Yang Z, Zhuo Y, Yuan R, Chai Y (2015) Amplified thrombin aptasensor based on alkaline phosphatase and hemin/G-quadruplex-catalyzed oxidation of 1-naphthol. *ACS Appl Mater Interfaces* 7(19):10308–10315
- Trapaidze A, Héroult JP, Herbert JM, Bancaud A, Gué A.M (2016) Investigation of the selectivity of thrombin-binding aptamers for thrombin titration in murine plasma. *Biosens Bioelectron* 78:58–66
- Wang L, Ma R, Jiang L, Jia L, Jia W, Wang H (2016) A novel signal-on/off sensing platform for selective detection of thrombin based on target-induced ratiometric electrochemical biosensing and bio-bar-coded nanoprobe amplification strategy. *Biosens Bioelectron* 92:390–395
- Deng N, Jiang B, Chen Y, Liang Z, Zhang L, Liang Y, Yang K, Zhang Y (2016) Aptamer-conjugated gold functionalized graphene oxide nanocomposites for human-thrombin specific recognition. *J Chromatogr A* 1427:16–21
- Du FK, Zhang H, Tan XC, Yan J, Liu M, Chen X, Wu YY, Feng DF, Chen QY, Cen JM, Liu SG, Qiu YQ, Han HY (2018) Ru(bpy)<sub>3</sub><sup>2+</sup>-Silica@Poly-L-lysine-Au as labels for electrochemiluminescence lysozyme aptasensor based on 3D graphene. *Biosens Bioelectron* 86:50–56
- Miao WJ (2008) Electrogenerated chemiluminescence and its biorelated applications. *Chem Rev* 108(7):2506–2553
- Chen X, Zhao L, Tian X, Lian S, Huang Z, Chen X (2014) A novel electrochemiluminescence tetracycline sensor based on a Ru(bpy)<sub>3</sub><sup>2+</sup>-doped silica nanoparticles/Nafion film modified electrode. *Talanta* 129:26–31
- Wu YY, Li XY, Tan XC, Yan J, Zhang H, Chen X, Huang ZY, Han HY (2018) A cyclic catalysis enhanced electrochemiluminescence aptasensor based 3D graphene/photocatalysts Cu<sub>2</sub>O-MWCNTs. *Electrochim Acta* 282:672–679
- Huang X, Yin ZY, Wu SX, Qi XY, He QY, Zhang QC, Yan QY, Boey F, Zhang H (2011) Graphene-based materials: synthesis, characterization, properties, and applications. *Small* 7:1876–1902, 14
- Li C, Shi GQ (2012) Three-dimensional graphene architectures. *Nanoscale* 4(18):5549–5563
- Qi YY, Li BX, Zhang ZJ (2009) Label-free and homogeneous DNA hybridization detection using gold nanoparticles-based chemiluminescence system. *Biosens Bioelectron* 24(12):3581–3586
- Robertson DL, Joyce GF (1990) Selection in vitro of an RNA enzyme that specifically cleaves single-stranded DNA. *Nature* 344(6265):467–468
- Mir M, Vreeke M, Katakis I (2006) Different strategies to develop an electrochemical thrombin aptasensor. *Electrochim Commun* 8(3):505–511
- Liu X, Freeman R, Golub E, Willner I (2011) Chemiluminescence and chemiluminescence resonance energy transfer (CRET) aptamer sensors using catalytic hemin/G-quadruplexes. *ACS Nano* 5(9):7648–7655
- Zhou Q, Lin Y, Lin Y, Wei Q, Chen G, Tang D (2016) In situ amplified electrochemical aptasensing for sensitive detection of adenosine triphosphate by coupling target-induced hybridization chain reaction with the assembly of silver nanotags. *Talanta* 146:23–28
- Ronkainen NJ, Halsall HB, Heineman WR (2010) Electrochemical biosensors. *Chem Soc Rev* 39(5):1747–1763

37. Khonsari YN, Sun SG (2017) Recent trends in electrochemiluminescence aptasensors and their applications. *Chem Commun* 53(65):9042–9054
38. Khonsari YN, Sun SG (2018) Electrochemiluminescent aptasensor for thrombin using nitrogen-doped graphene quantum dots. *Microchim Acta* 185(9):430
39. Marcano DC, Kosynkin DV, Berlin JM, Sinitskii A, Sun Z, Slesarev A, Alemany LB, Lu W, Tour JM (2010) Improved synthesis of graphene oxide. *ACS Nano* 4(8):4806–4814
40. Yuan WJ, Li JC, Chen P, Shen YH, Xia AJ (2014) A one-pot hydrothermal synthesis of 3D nitrogen-doped graphene aerogels-supported NiS<sub>2</sub> nanoparticles as efficient electrocatalysts for the oxygen-reduction reaction. *J Nanopart Res* 16(3):2311
41. Sun X, Du Y, Zhang LX, Dong SJ, Wang EK (2006) Pt nanoparticles: heat treatment-based preparation and Ru(bpy)<sub>3</sub><sup>2+</sup>-mediated formation of aggregates that can form stable films on bare solid electrode surfaces for solid-state electrochemiluminescence detection. *Anal Chem* 78(18):6674–6677
42. Chen S, Song Y, Li Y, Liu Y, Su X, Ma Q (2015) A facile photoluminescence modulated nanosensor based on nitrogen-doped graphene quantum dots for sulfite detection. *New J Chem* 39(10):8114–8120
43. Lu JJ, Yan M, Ge L, Ge SG, Wang SW, Yan JX, Yu JH (2013) Electrochemiluminescence of blue-luminescent graphene quantum dots and its application in ultrasensitive aptasensor for adenosine triphosphate detection. *Biosens Bioelectron* 47:271–277
44. Li Y, Zhao Y, Cheng HH, Hu Y, Shi GQ, Dai LM, Qu LT (2012) Nitrogen-doped graphene quantum dots with oxygen-rich functional groups. *J Am Chem Soc* 134(1):15–18
45. Cai Z, Li F, Wu P, Ji L, Zhang H, Cai C, Gervasio DF (2015) Synthesis of nitrogen-doped graphene quantum dots at low temperature for electrochemical sensing trinitrotoluene. *Anal Chem* 87(23):11803–11811
46. Huang HP, Zhu JJ (2009) DNA aptamer-based QDs electrochemiluminescence biosensor for the detection of thrombin. *Biosens Bioelectron* 25(4):927–930
47. Xing HH, Zhai QF, Zhang XW, Li J, Wang E.K (2018) Boron nitride quantum dots as efficient coreactant for enhanced electrochemiluminescence of ruthenium(II) tris(2,2'-bipyridyl). *Anal Chem* 90:2141–2147, 3
48. Liu Y, Liu N, Ma X, Li X, Ma J, Li Y, Zhou Z, Gao Z (2015) Highly specific detection of thrombin using an aptamer-based suspension array and the interaction analysis via microscale thermophoresis. *Analyst* 140(8):2762–2770
49. Duan WN, Wang XZ, Wang HX, Li F (2018) Fluorescent and colorimetric dual-mode aptasensor for thrombin detection based on target-induced conjunction of split aptamer fragments. *Talanta* 180:6–80
50. Radi A, Sanchez JL, Baldrich E, O'sullivan CK (2006) Reagentless, reusable, ultrasensitive electrochemical molecular beacon aptasensor. *J Am Chem Soc* 128:117–124, 1
51. Chen Q, Chen H, Zhao YY, Zhang F, Yang F, Tang J, He PG (2014) A label-free electrochemiluminescence aptasensor for thrombin detection based on host-guest recognition between tris(bipyridine)ruthenium (II)-beta-cyclodextrin and aptamer. *Biosens Bioelectron* 54:547–552

**Publisher's note** Springer Nature remains neutral with regard to jurisdictional claims in published maps and institutional affiliations.